5.1 Entrainment and Mixing in Small Cumulus Clouds

Alan M. Blyth*
University of Leeds, Leeds, United Kingdom

Sonia G. Lasher-Trapp
New Mexico Tech, Socorro, New Mexico

William A. Cooper
National Center for Atmospheric Research†
Boulder, Colorado

1 INTRODUCTION

The purpose of this study is to examine how dry environmental air is entrained into small cumulus clouds and how that air is mixed into the cloud. It is motivated by our study into whether the cloud droplet size distribution can be explained by supersaturation variations along trajectories (Lasher-Trapp et al 2002).

Studies of mixing of dry environmental air with cloudy air by Austin et al. (1985) and Paluch and Baumgardner (1989), for example, have shown that there are essentially three types of regions in a cumulus cloud: (1) unmixed; (2) actively mixing; and (3) well mixed. Austin et al. found that "variable" and "steady" regions were often separated by transition zones of less than ten metres. Krueger et al. (1997) described a conceptual picture of mixing that is consistent with the process examined by Broadwell and Breidenthal (1982) in the laboratory and the observations of fine-scale mixing by Paluch and Baumgardner (1989). Eddies capture dry environmental air and the entrained air is wrapped up in the eddy until the Kolmogorov scale when the layers are thin and the interface is large. Molecular mixing then becomes efficient and the cloud droplets come in close proximity to the environmental air. The time scale of this complete homogenization is of the order $(l^2/\epsilon)^{1/3}$ where l is the initial size of the eddy and ϵ is the eddy dissipation rate. A typical time to reach the Kolmogorov scale is about 100 s for typical values of $l = 100$ m and $\epsilon = 10^{-2}$ m^{2}s^{-3}.

Carpenter et al. (1998) used a cloud model with 50 m resolution to examine the entrainment process in New Mexican cumulus clouds which are well known for being multi-thermal in nature. Their model results suggested that thermals were responsible for most of the entrainment and detrainment. They found general agreement with the Blyth, Cooper and Jensen (1988; hereafter BCJ) schematic model of a single-thermal cumulus cloud: undiluted boundary layer air existed at all levels of the cloud; the core eroded as the thermal ascended; air was entrained at the front of the thermal and was then swept either back into the rear or into the trailing wake. Entrainment also occurred laterally through the sides, which is a deviation from the BCJ picture. The resolution used in the runs was not sufficiently high to determine whether or not entrainment occurred via turbulent eddies at the front or side interface of the thermal. The edges were generally smooth, similar to those in laboratory thermals (e.g. Sanchéz et al. 1989).

Grabowski and Clark (1993) (hereafter GC) performed 3-D numerical simulations of an ascending thermal with a resolution of 3.125 m and 6.25 m. They concluded that entrainment in convective clouds with high Reynolds number is dominated by structures which develop as a result of perturbations in the buoyancy at the interface. Not surprisingly, they found that buoyant production of kinetic energy (KE) was found to be largest near the thermal top while shear production dominated near the side. The competing mechanisms are the

* *Corresponding author address*: Alan M. Blyth, Institute of Atmospheric Science, School of Environment, University of Leeds, Leeds, LS2 9JT, UK; e-mail: a.m.blyth@leeds.ac.uk

† NCAR is supported by the National Science Foundation

sharpening of gradients of thermodynamic fields and momentum by the continued rise of the thermal, and the smoothing out of these gradients by the large-scale instabilities which develop at the upper edge of the thermal. This defines the depth of the mixing region which should be constant in time when averaged over times longer than the lifetime of a large eddy if these two processes are in balance. GC estimated that the quasi-equilibrium depth of the mixing region as $l_{eq} \sim R/10$ where R is the radius of the thermal; this defines a typical eddy size. They therefore concluded that entrainment in cumulus clouds is dominated by large structures (with size l_{eq}) developing at the interface.

2 PREDICTIONS

There appears to be two dominant scales of motion therefore: the circulation on the thermal scale R with turbulent eddies of size l_{eq} at the cloud edges. The dilution of a cumulus turret occurs as entrained air from the top and sides of the turret enters through the rear. According to this BCJ and CG conceptual picture, instruments on an aircraft which penetrates through the main region of a thermal would measure: downdrafts at the edges with low values of liquid water content L; eddies on scales of about l_{eq} at the edge of the updraft; a sharp increase in L at the transition between downdraft and updraft, but also high variation in L for a distance of no more than about l_{eq} from the interface; divergence of the updraft; and large and smooth liquid water content in the updraft.

Of course, vertical wind shear and turbulent fluctuations in buoyancy will distort the simple picture. In fact, it can be difficult to extrapolate observations of air velocity made with an aircraft to the 3D motions in a cumulus cloud. Fig. 1 shows a vertical slice from the model used by Carpenter et al. (1998) and run by Lasher-Trapp et al. (2001) for a cloud measured during SCMS on 22 July 1995. The figure illustrates the gross features mentioned above, but they also show the complication of the wind field compared to a relatively simple profile of liquid water content, L. If measurements were made at about 3.1 km it would be difficult to conclude that the winds measured were part of a thermal circulation. There is clear evidence in the model cross-section however of an updraft, edge downdrafts, air entering the rear of a distorted thermal and vorticity on both sides. The maximum lwc (which is greater than 80% of the adiabatic value) does not coincide with the maximum updraft at this time in the simulation. Notice the sharp gradient in both L and vertical wind w on one side and the smoother gradients on the other side.

3 THERMALS

There is growing evidence for thermals in cumulus clouds as discussed below.

- There have been observations of undiluted regions at all altitudes reported in the literature (e.g. Jensen et al. 1985). The fact that such regions are observed during a small percentage of the total number of penetrations is consistent with the thermal model.

- The normalized width of core regions have been observed to decreases with altitude.

- Downdrafts have frequently been observed on either side of updrafts. Kollias et al. (2001) for example showed an excellent case of a small cumulus cloud observed with a 94 GHz cloud radar and 915 MHz wind profiler. Fig. 2 shows data from a penetration through three small Florida cumulus clouds at 2 km on 6 August 1995. There are downdrafts on either side of the updraft and the values of $\Delta v_x/\Delta x$ show strong divergence within each turret. Notice that $\Delta v_x/\Delta x$ is negative in the downdrafts. Divergence is often observed in the updraft (e.g. BCJ), although this has not been reported frequently in the literature.

- Strong inflow with concomitant lower liquid water content following a thermal has been observed by BCJ. This would be observed more frequently if there was entrainment laterally across the entire turret. The fact that such inflow is rarely observed supports the thermal picture.

- Stith (1992) released the tracer hexafluoride near cloud top a and later observed it significantly below cloud top and extending into the centre of the cloud.

- Observations of "inverted cup echoes" have been made with S-band radars for many years. The Bragg scattering signal is greater when there are fluctuations in the liquid water and temperature fields (on a scale of half the wavelength). This is significant since it clearly

shows that the region of active mixing does not extend into the centre of the cloud.

- Reduced liquid water content has occasionally been observed in the region of a turret with the strongest updraft and divergence. It is puzzling why this is not observed more frequently.

Thus, there is general support for the general thermal picture suggested by BCJ. What is missing is information on the details of how air is entrained into the edge of thermals.

4 CLOUD EDGES

A study of several penetrations made in single SCMS clouds above 1 km shows that there was an increase in the liquid water content of at least 0.02 g m^{-3} m^{-1} at the cloud edge in over 75% of the penetrations examined. Maximum values were almost an order of magnitude higher. The gradient of the vertical wind at the edge of the updraft was at least 0.2 m s^{-1} m^{-1} in slightly over half of the upshear sides of the penetrations examined, with a maximum value of about 1.0 m s^{-1} m^{-1}. Fig 3 shows the gradient of L at the left and right edges of small cumulus clouds on 10 August plotted against the maximum updraft measured in that cloud. The gradients were calculated with the 10 Hz FSSP data from zero to the point where the liquid wtaer content first stopped increasing. Gradients may be even sharper if the 1 kHz Gerber probe data are used. These data will be examined in future work. Notice that the largest gradient is about 0.15 g m^{-3} m^{-1}. There is no tendency for the gradient to increase with updraft speed. One edge is sharper than the other in the majority of clouds.

Fig. 4 shows a penetration through a SCMS cloud on 28 July 1995. Many features are typical of several other penetrations, although the updraft is somewhat stronger than normal. The time series of liquid water content and vertical wind are similar to the model values shown in Fig. 1. The liquid water content increases sharply from zero to the highest value on one side of the cloud, but decreases gradually to zero on the other side. The gradient of the vertical wind, $\Delta w/\Delta x$, also shown in the figure, has a maximum of about 0.5 m s^{-1} m^{-1} in small regions very close to both edges. The gradient at the left edge is about 0.1 m s^{-1} m^{-1}. This is the normal shear at the thermal interface mentioned by CG (assuming the aircraft enters the side of the cloud). The other quantity of interest is the departure from parallel shear flow near the interface, $\Delta v_x/\Delta x$ which is shown in the second panel of the figure. There are clearly large values of this quantity near both edges.

A pertinent question is how frequently do eddies form at the edge of the updraft and is their size of the order of l_{eq}? Wavelet analysis (Torrence and Compo 1998) will be used in future work in order to examine this question in detail. As mentioned above, models have to achieve the right balance of the production of gradients by the ascent of the thermal and the destruction of these gradients by mixing. Are there large gradients in w more often than models predict, or are turbulent eddies more common than models predict? Other indications of the presence of turbulent eddies are a rapid change in the direction of v_x across the eddy and high variability in L. Scaling arguments mentioned above suggest $l_{eq} \sim 100$ m. An eddy (or eddies) with size about 100 m can be seen form the inward pointing wind vectors at the left edge of the updraft and from the variations in the 1 kHz liquid water content shown in Fig. 4. Eddies such as this are commonly observed. We aim to characterise these, and cloud edges in general, in future work.

Acknowledgements This work was supported in part by the National Science Foundation under grant no. ATM-9981937.

5 REFERENCES

Austin, P. H., M. B. Baker, A. M. Blyth, and J. B. Jensen, 1985: Small-scale variability in warm continental cumulus clouds. *J. Atmos. Sci.*, **42**, 1123 - 1138.

Blyth, A. M., W. A. Cooper, and J. B. Jensen, 1988: A study of the source of entrained air in Montana cumuli. *J. Atmos. Sci.*, **45**, 3944 - 3964.

Broadwell, J. E., and R. E. Breidenthal, 1982: A simple model of mixing and chemical reaction in a turbulent shear layer. *J. Fluid Mech.*, **125**, 397 - 410.

Carpenter, R. L., K. K. Droegemeier, and A. M. Blyth, 1998: Entrainment and detrainment in numerically simulated cumulus congestus clouds. Part III: Detailed Analysis of Specific Events. *J. Atmos. Sci.*, **55**, 3440 - 3455.

Grabowski, W. W., and T. L. Clark, 1993: Cloud-environment interface instability. Part II: Extension to three spatial dimensions. *J. Atmos. Sci.*, **50**, 555 - 573.

Jensen, J. B., P.H. Austin, M.B. Baker and A.M. Blyth, 1985: Turbulent mixing, spectral evolution and dynamics in a warm cumulus cloud. *J. Atmos. Sci.*, **42**, 173 - 192.

Kollias, P., B. A. Albrecht, R. Lhermitte, and A. Savtchenko, 2001: Radar observations of updrafts, downdrafts, and turbulence in fair-weather cumuli. *J. Atmos. Sci.*, **58**, 1750 - 1766.

Krueger, S. K., C-W. Su, and P. A. McMurtry, 1997: Modeling entrainment and finescale mixing in cumulus clouds. *J. Atmos. Sci.*, **54**, 2697 - 2712.

Lasher-Trapp, S. G., C. A. Knight, and J. M. Straka, 2001: Early radar echoes from ultragiant aerosol in a cumulus congestus: Modeling and observations. *J. Atmos. Sci.*, **58**, 3545 - 3562.

Lasher-Trapp, S.G., W.A. Cooper and A.M. Blyth, 2002: *Proc 11th AMS Conf on Cloud Physics*, This volume.

Paluch, I. R., D. Baumgardner, 1989: Entrainment and fine-scale mixing in a continental convective cloud. *J. Atmos. Sci.*, **46**, 261 - 278.

Sánchez, O., D. J. Raymond, L. Libersky, A. G. Petschek, 1989: The development of thermals from rest. *J. Atmos. Sci.*, **46**, 2280 - 2292.

Stith, J. L., 1992: Observations of cloud-top entrainment in cumuli. *J. Atmos. Sci.*, **49**, 1334-1347.

Torrence, C., and G. P. Compo, 1998: A practical guide to wavelet analysis. *Bull. Amer. Meteor. Soc.*, **79**, 61 - 78.

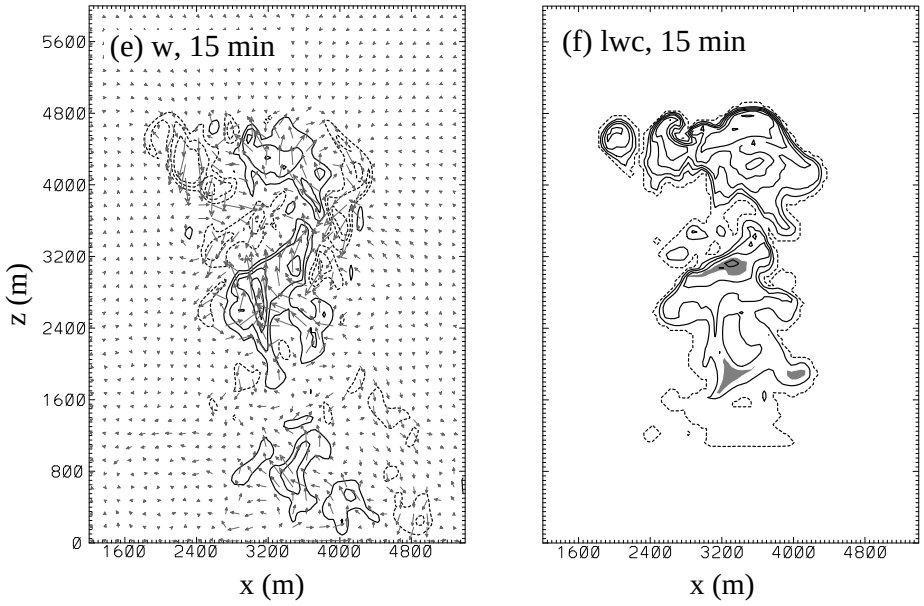

Figure 1: *Vertical cross sections of model simulated vertical velocity (left) and lwc (right) for 15 min run time (see text). Contour interval for vertical velocity is 2 m* s^{-1} *and for liquid water content is 1 g* m^{-3}*. Dashed countours denote negative values for vertical velocity plots and cloud boundary (0.001 g* m^{-3}*) for cloud water plots. (From Lasher-Trapp et al. 2001).*

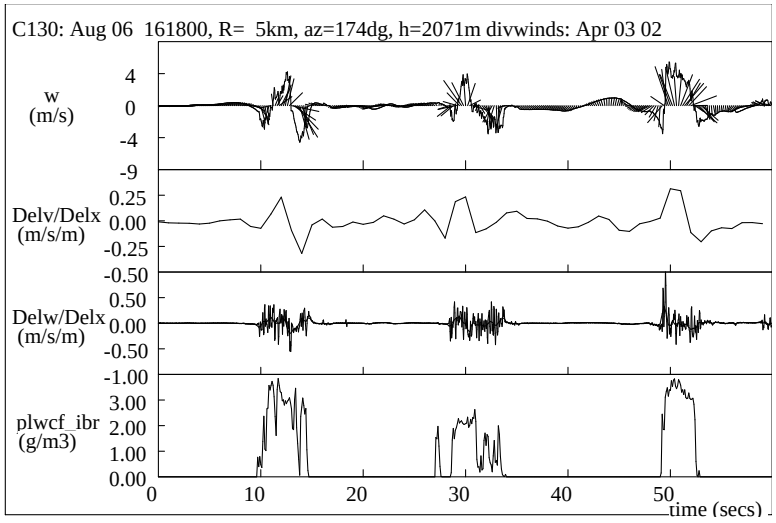

Figure 2: *Date gathered during a penetration of a cloud on 6 Aug 1995 at 2 km MSL. The top panel is the vertical wind with vectors produced from the vertical wind and component of the horizontal wind along the aircraft track. The second panel is 10 times the 1-s averaged values of* $\Delta v_x/\Delta x$*. The third panel is 25 Hz* $\Delta w/\Delta x$ *with 5 Hz average superimposed and the bottom panel is the 1000 Hz Gerber probe liquid water content.*

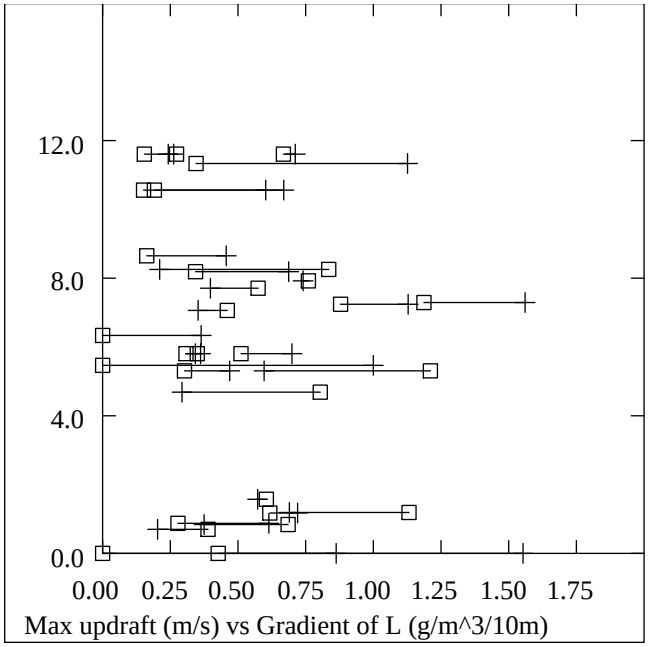

Figure 3: $\Delta L/\Delta x$ *at the edge of turrets plotted against the maximum updraft speed measured in that turret for SCMS clouds on 10 August 1995. The left and right edges are joined by a horizontal line. 10 Hz FSSP data were used in the calculation.*

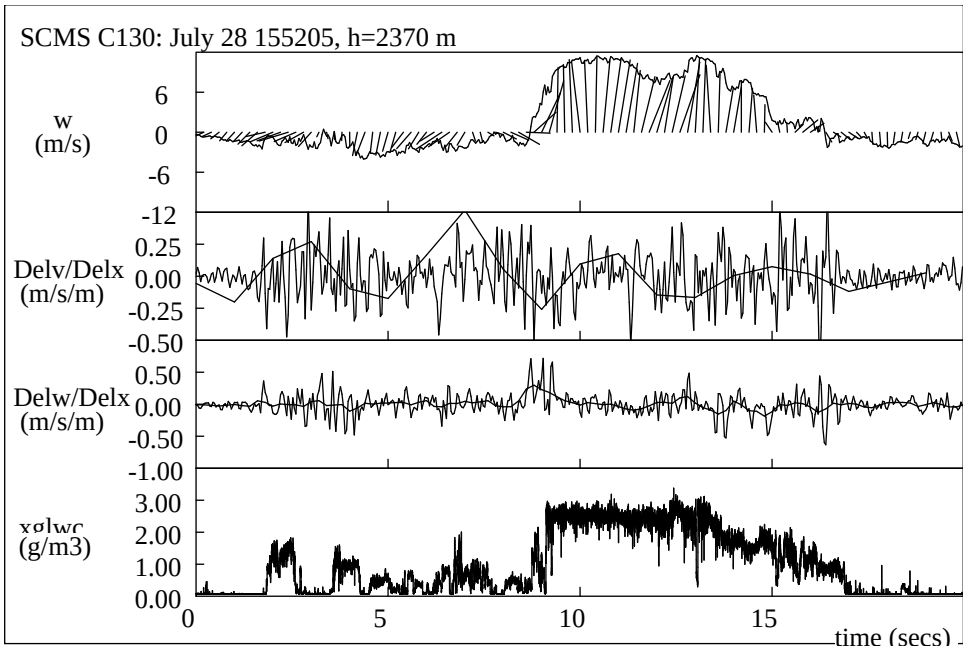

Figure 4: *Date gathered during a penetration of a cloud on 28 July 1995. The top panel is the vertical wind with vectors produced from the vertical wind and component of the horizontal wind along the aircraft track. The second panel is 25 Hz* $\Delta v_x/\Delta x$ *with 10 times the 1 Hz average superimposed. The third panel is 25 Hz* $\Delta w/\Delta x$ *with 5 Hz average superimposed. The bottom panel is the 1000 Hz Gerber probe liquid water content.*